Self-Similar One-Dimensional Quasilattices

Latham Boyle,[a] **Paul J. Steinhardt**[a,b,c]

[a]*Perimeter Institute for Theoretical Physics,*
Waterloo, Ontario N2L 2Y5, Canada

[b]*Princeton Center for Theoretical Science, Princeton University*
Princeton, NJ, 08544 USA

[c]*Department of Physics, Princeton University*
Princeton, NJ, 08544 USA

ABSTRACT: We study 1D quasilattices, especially self-similar ones that can be used to generate two-, three- and higher-dimensional quasicrystalline tesselations that have matching rules and invertible self-similar substitution rules (also known as inflation rules) analogous to the rules for generating Penrose tilings. The lattice positions can be expressed in a closed-form expression we call *floor form*: $x_n = S(n - \alpha) + (L - S)\lfloor \kappa(n - \beta) \rfloor$, where $L > S > 0$ and $0 < \kappa < 1$ is an irrational number. We describe three equivalent geometric constructions of these quasilattices and show how they can be subdivided into various types of equivalence classes: (i) *lattice equivalent*, where any two quasilattices in the same lattice equivalence class may be derived from one another by a local decoration/gluing rule; (ii) *self-similar*, a proper subset of lattice equivalent where, in addition, the two quasilattices are locally isomorphic; and (iii) *self-same*, a proper subset of self-similar where, in addition, the two quasilattices are globally isomorphic (*i.e.* identical up to rescaling). For all three types of equivalence class, we obtain the explicit transformation law between the floor form expression for two quasilattices in the same class. We tabulate (in Table 1 and Figure 5) the ten special self-similar 1D quasilattices relevant for constructing Ammann patterns and Penrose-like tilings in two dimensions and higher, and we explicitly construct and catalog the corresponding self-same quasilattices. Finally, we sketch the extension of our results from degree two to degree N (*i.e* to 1D quasilattices built from N different intervals).

Contents

1 Introduction

Penrose tilings [1–3] were the inspiration for introducing the concept of quasicrystals [4] and have stimulated enormous progress in our understanding of aperiodic order in mathematics and physics [5–10]. These tilings exhibit a fascinating set of interrelated properties, including: (i) quasiperiodic translational order; (ii) crystallographically-forbidden 10-fold orientational order; (iii) discrete scale invariance (as embodied in so-called "inflation/deflation" rules [2]); (iv) "matching" rules that constrain the way two tiles can join edge-to-edge such that the tiles can only fill the plane by forming perfect Penrose tilings; and (v) a distinctive class of topological ("decapod") defects. The Penrose tiles also have another important feature: the two tiles can each be decorated with a certain pattern of line segments that join together in a perfect Penrose tiling to form five infinite sets of parallel lines oriented along the five edges of a pentagon. The lines are spaced according to a 1D quasiperiodic sequence of long and short intervals called a "Fibonacci quasilattice" (see Fig. 1). The five sets of 1D quasilattices collectively form an Ammann pattern, named after Robert Ammann, who first noted this decoration [5, 11].

    In this paper we lay the 1D foundation for a new approach to Penrose tilings (and other objects like them, but with different symmetries and in higher dimensions) [12]. The perspective developed and applied in [12] is that a Penrose-like tiling should be regarded
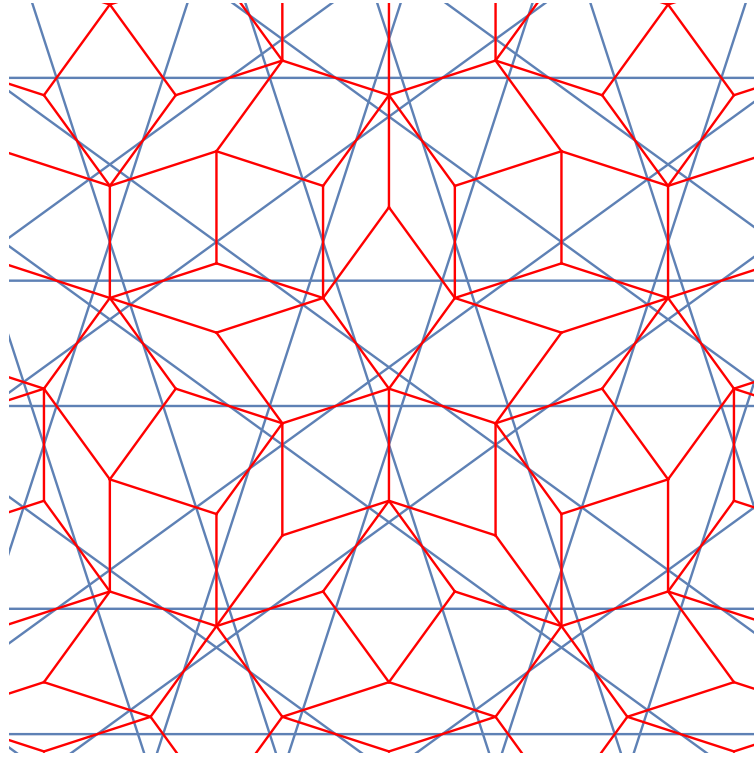
Figure 1. The red lines show a portion of a Penrose tiling (constructed from two tiles – a thin rhomb and a fat rhomb), while the blue lines show the corresponding Ammann pattern.

as the dual of a more fundamental object: an Ammann pattern; and this Ammann pattern, in turn, can be derived from the relationship between two naturally-paired irreducible reflection groups (which we call a "Coxeter pair").

Our focus in this paper is the analysis of the 1D quasilattices that serve as the building blocks for the Ammann patterns in higher dimensions. Although our ultimate purpose is higher-dimensional quasicrystal tilings as described in [12], the 1D quasilattices studied here are important objects in their own right (see *e.g.* [7, 10, 13–19]), and a number of the new results about them that we present here are of independent interest. Let us sketch the outline of this paper and highlight a few of the key results:

We begin, in Section 2, by constructing the simplest class of 1D quasilattices: we will call them "1D quasilattices of degree two" or "quadratic 1D quasilattices". These are 1D quasiperiodic lattices constructed from just two intervals or "tiles" (call them L and S, for "long" and "short"), with just two different separations between successive L's, and just two different separations between successive S's (the simplest possibility compatible with quasiperiodicity). The quasilattice point positions can be specified by a closed-form analytic expression which has the basic "floor form" $x_n = S(n - \alpha) + (L - S)\lfloor \kappa(n - \beta) \rfloor$ where $\lfloor x \rfloor$ denotes the "floor of x" (*i.e.* the largest integer $\leq x$) and $L > S > 0$, α, β and $0 < \kappa < 1$ are constants.

The quasilattices can be constructed geometrically by first picking some input data:

an arbitrary 2D lattice Λ, an integral basis $\{\vec{m}_1, \vec{m}_2\}$ for Λ, and an arbitrary line $\vec{q}(t)$ that slices through the lattice with irrational slope. We describe three equivalent constructions that produce the natural 1D quasilattice corresponding to this input data: (i) the first construction involves dualizing the "1D bi-grid" obtained by intersecting the $\{\vec{m}_1, \vec{m}_2\}$ integer grid lines with the line $\vec{q}(t)$; (ii) the second construction is based on a cut-and-project scheme using Λ as the lattice, $\vec{q}(t)$ as the "cut" surface, and a parallelogram with sides $\vec{m}_1$ and $\vec{m}_2$ as the acceptance window; and (iii) the third construction is based on thinking about the 2-torus $\mathbb{T}$ defined by considering the 2D Euclidean plane modulo Λ: $\vec{q}(t)$ then becomes a geodesic which wraps around and around $\mathbb{T}$, densely covering its surface, and the quasilattice corresponds to the intersection of $\vec{q}(t)$ with an appropriate perpendicular cross-cut of $\mathbb{T}$. At first glance, it might seem like the first (dualization) construction only defines the 1D quasilattice up to an overall (unfixed) translational phase ambiguity; but it will be important for later applications [12] to remove this phase ambiguity by imposing the condition that the 1D bi-grid is reflection symmetric if and only if the corresponding 1D quasilattice is reflection symmetric. We then observe that this condition has a natural geometric interpretation in the second (cut-and-project) construction: it amounts to the requirement that, whenever the line $\vec{q}(t)$ intersects one of the $\{\vec{m}_1, \vec{m}_2\}$ parallelograms in the lattice Λ, it is the *midpoint* of that parallelogram that should be projected onto $\vec{q}(t)$ to define a point in the 1D quasilattice. We show [see (2.11) or (2.14)] that these three geometric constructions yield 1D quasilattices captured by the floor-form expression described above; and, conversely, that any 1D quasilattice in floor-form (for any values of the parameters S, L, α, β and κ) can be obtained via these geometric constructions.

Section 3 is about the following simple observation. In Section 2, we began by choosing a line $\vec{q}(t)$, a lattice Λ, and an integral basis $\{\vec{m}_1, \vec{m}_2\}$ for Λ; and we obtained a corresponding 1D quasilattice x_n. But the choice of integral basis $\{\vec{m}_1, \vec{m}_2\}$ for Λ was not unique, and if we had instead chosen a different integral basis $\{\vec{m}'_1, \vec{m}'_2\}$ and otherwise followed the same construction, we would have obtained a different quasilattice x'_n. We will say that two such quasilattices are "lattice equivalent": x_n and x'_n might look quite dissimilar from one another, in terms of their tile sizes and orderings, but (as we explain in Section 3) they are secretly equivalent to one another in the sense that each one may be obtained from the other by a local "substitution/gluing" rule – in particular, one may be obtained as a local *decoration* of the other in the sense that the first can be obtained by subdividing each type interval of the second into a specific sequence of smaller intervals, with this substitution/decoration rule precisely corresponding to the invertible integer 2×2 matrix τ which relates the old basis $\{\vec{m}_1, \vec{m}_2\}$ to the new basis $\{\vec{m}'_1, \vec{m}'_2\}$. In this way, the set of quadratic 1D quasilattices is partitioned into "lattice equivalence classes" with a simple geometric interpretation: the members of a given class correspond to the same line $\vec{q}(t)$ and the same lattice Λ, but different choices for the basis $\{\vec{m}_1, \vec{m}_2\}$.

In Section 4, we identify the subset of quadratic 1D quasilattices that are *self-similar*. For these lattices, there is a change of basis $\{\vec{m}_1, \vec{m}_2\} \to \{\vec{m}'_1, \vec{m}'_2\}$ that maps the quasilattice x_n into a new quasilattice x'_n that is not only lattice equivalent, but also *locally isomorphic* up to rescaling of the intervals between points. For each self-similar 1D quasilattice, our construction identifies a canonical self-similar substitution/decoration rule, specifying

not just the *number* of "new" tiles which decorate each of the "old" tiles, but also the particular order and phase of the new tiles in decorating the old. This canonical substitution rule is always reflection symmetric. We also obtain a simple and useful analytic expression for how the parameters in the floor-form expression for the "old" quasilattice are related to the parameters in the floor-form expression for the "new" quasilattice obtained from it by this canonical substitution rule. In a generic (non-singular) self-similar quasilattice, the line $\vec{q}(t)$ does not intersect any of the points in the lattice Λ; but we also carefully treat the special (singular) case where $\vec{q}(t)$ does intersect a point in Λ, because the corresponding special quasilattices play an important role in the analysis of topological defects in Penrose-like tilings in two dimensions and higher [20]. Finally, since we are dealing with quadratic 1D quasilattices, the corresponding self-similar quasilattices are characterized by quadratic irrationalities. In fact, only a small subset of these self-similar quadratic 1D quasilattices play a role as the building blocks for the Ammann patterns in two dimensions and higher [12]: the parameters and canonical substitution rules for these ten special quasilattices are presented in Table 1 and Figure 5.

In Section 5, we identify the subset of quadratic 1D quasilattices that are not only self-similar under some 2×2 transformation τ, but are exactly *s-fold self-same*; that is, τ^s maps the quasilattice x_n to a new quasilattice x'_n that is not merely locally-isomorphic, but actually *identical* to the original quasilattice (up to an overall rescaling). We obtain a simple explicit formula for these s-fold self-same quasilattices, and also for the *number* of distinct s-fold self-same quasilattices. These s-fold self-same quasilattices are naturally grouped into irreducible s-cycles: for each of the special quasi-lattices listed in Table 1, we count the number of irreducible s-cycles, and list the results in Table 2. In comparing the results to the Online Encyclopedia of Integer Sequences (OEIS), some interesting connections appear. These s-fold self-same 1D quasilattices, and irreducible s-cycles thereof, are the building blocks for s-fold self-same Ammann patterns and Penrose-like tilings in two dimensions and higher; and these, in turn, underlie a new scheme for discretizing scale invariant systems.

Finally, in Section 6, we briefly discuss the generalization of our results from quadratic 1D quasilattices (which are produced by a 2D→1D cut-and-project algorithm, and contain two different intervals) to 1D quasilattices of degree N (which are produced by an ND→1D cut-and project algorithm, and contain N different intervals).

2 Quadratic 1D quasilattices: three geometric perspectives

We will say that a 1D quasilattice is "of degree two" or "quadratic" if it can be described by the following "floor form" expression:

$$x_n = S(n - \alpha) + (L - S)\lfloor \kappa(n - \beta) \rfloor. \tag{2.1}$$

Here $\{L, S, \kappa, \alpha, \beta\}$ are real-valued constants (with $L > S > 0$ and $0 < \kappa < 1$ irrational), n is an integer that runs from $-\infty$ to $+\infty$, and $\lfloor x \rfloor$ is the "floor" of x (*i.e.* the greatest integer $\leq x$). Thus, as n increases (from N to $N + 1$), x_n correspondingly increases (from x_N to either $x_{N+1} = x_N + L$ or $x_{N+1} = x_N + S$); in other words, Eq. (2.1) describes a sequence of isolated points along the real line, with just two different intervals between neighboring

points: L and S ("long" and "short"). The L's and S's form an infinite non-repeating sequence: the relative frequency with which L and S occur in the sequence is determined by κ and the particular order in which they occur is determined by β, while α is an overall translation phase that determines where exactly the sequence is situated along the real line.

Note that quadratic 1D quasilattices are "as simple as possible" in the sense that they are built from just two different intervals (L and S); and, in addition, there are just two different separations between consecutive S's, and just two different separations between consecutive L's. Anything simpler that this would be incompatible with quasiperiodicity.

In this section, we present three equivalent geometric constructions of all such quadratic 1D quasilattices. Our formulation is designed to clarify the relationship between cut-and-project sequences, on the one hand, and lattice equivalence, self-similarity and self-sameness, on the other. In the process, we obtain a number of explicit expressions that will be needed in subsequent sections, and in our construction of higher-dimensional Ammann patterns in [12].

The starting point for all three constructions is the same: an arbitrary Bravais lattice Λ in 2D Euclidean space sliced by an arbitrary line $\vec{q}(t)$; and a choice of a "positive" integer basis $\{\vec{m}_1, \vec{m}_2\}$ for Λ. We begin, then, by introducing these three ingredients.

2.1 Geometric preliminaries: the lattice Λ, the line $\vec{q}(t)$, and the basis $\{\vec{m}_1, \vec{m}_2\}$

Let Λ be an arbitrary lattice in 2D Euclidean space, and let $\{\vec{m}_1, \vec{m}_2\}$ be a (not necessarily orthonormal) integer basis for the lattice: *i.e.* every point in Λ may be written as a unique integer linear combination of the vectors $\vec{m}_1$ and $\vec{m}_2$. If we regard $\vec{m}_1$ and $\vec{m}_2$ as column vectors, then the corresponding dual basis $\{\widetilde{m}^1, \widetilde{m}^2\}$ consists of the row vectors $\widetilde{m}^1$ and $\widetilde{m}^2$ defined by the matrix equation

$$\begin{bmatrix} \widetilde{m}^1 \\ \widetilde{m}^2 \end{bmatrix} = [\, \vec{m}_1 \;\; \vec{m}_2 \,]^{-1} \qquad \Rightarrow \qquad \widetilde{m}^i \vec{m}_j = \delta^i{}_j. \tag{2.2}$$

Let $\vec{q}(t)$ be an arbitrary line slicing through this space, and let $\{\hat{e}_\parallel, \hat{e}_\perp\}$ be an orthonormal basis adapted to it: $\hat{e}_\parallel$ points along the line, $\hat{e}_\perp$ points perpendicular to it, and we write:

$$\vec{q}(t) = \vec{q}_0 + \hat{e}_\parallel t. \tag{2.3}$$

We will always assume that $\vec{q}(t)$ has irrational slope with respect to the $\{\vec{m}_1, \vec{m}_2\}$ basis. It will be convenient to split $\vec{q}_0$, $\vec{m}_1$ and $\vec{m}_2$ into their $\hat{e}_\parallel$ and $\hat{e}_\perp$ components:

$$\vec{q}_0 \; = \; q_0^\parallel \hat{e}_\parallel + \; q_0^\perp \hat{e}_\perp, \tag{2.4a}$$

$$\vec{m}_1 = m_1^\parallel \hat{e}_\parallel + m_1^\perp \hat{e}_\perp. \tag{2.4b}$$

$$\vec{m}_2 = m_2^\parallel \hat{e}_\parallel + m_2^\perp \hat{e}_\perp. \tag{2.4c}$$

In this paper, we will usually focus on the case where $\{\vec{m}_1, \vec{m}_2\}$ is a "positive basis," meaning that (for $i = 1, 2$) it satisfies the following conditions

$$\widetilde{m}^i \hat{e}_\parallel > 0, \tag{2.5a}$$

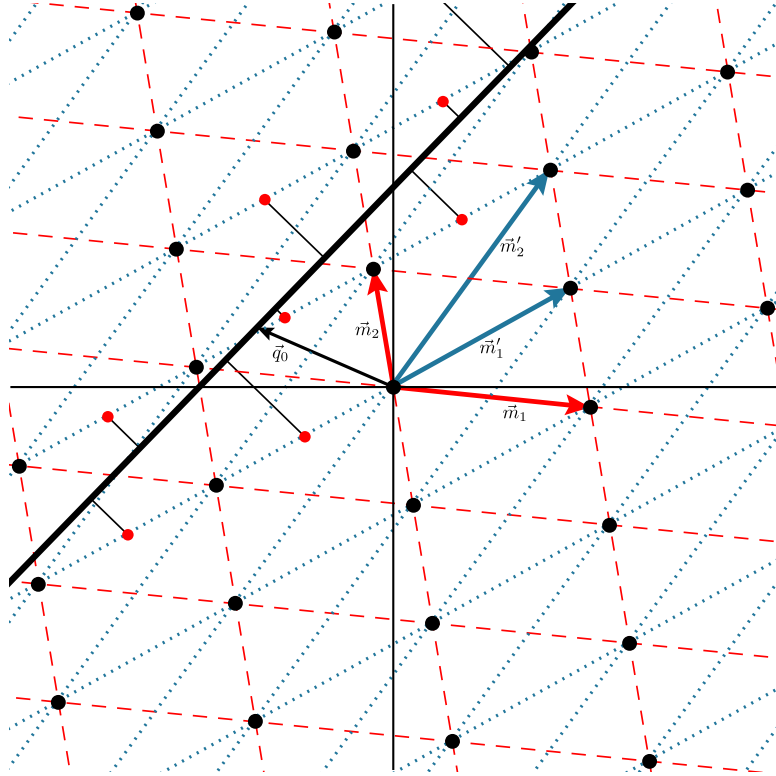$$\vec{m}_i \cdot \hat{e}_\parallel > 0. \tag{2.5b}$$

Figure 2. Illustrates the geometric objects discussed in Sections 2 and 3. The black dots are the lattice Λ. The thick black line is $\vec{q}(t)$, with its own origin displaced from the origin of Λ by the vector $\vec{q}_0$. The solid red arrows show an integer basis $\{\vec{m}_1, \vec{m}_2\}$ for Λ, while the dashed red lines show the corresponding integer grid; and the figure illustrates the corresponding cut-and-project construction: every time the solid black line $\vec{q}(t)$ intersects one of the red dashed parallelograms, the midpoint of that parallelogram (a red dot) is orthogonally projected onto $\vec{q}(t)$ to obtain the 1D quasilattice x_n. The solid turquoise arrows then show an alternative integer basis $\{\vec{m}_1', \vec{m}_2'\}$ for Λ, while the dotted turquoise lines show the corresponding integer grid; and this alternative basis could be used in an exactly analogous way to obtain a second quasilattice x_n' which would be in the same equivalance class as the first: either one could be obtained from the other by a local decoration/gluing rule.

In other words, Eq. (2.5a) says that the vector $\hat{e}_\parallel$ lies in the "first quadrant" with respect to the $\{\vec{m}_1, \vec{m}_2\}$ basis (*i.e.* if we expand $\hat{e}_\parallel = \alpha_1 \vec{m}_1 + \alpha_2 \vec{m}_2$ in the $\{\vec{m}_1, \vec{m}_2\}$ basis, then the coordinates α_1 and α_2 are both positive); and Eq. (2.5b) says that $\vec{m}_1$ and $\vec{m}_2$ both have positive projections onto $\hat{e}_\parallel$ (*i.e.* $m_1^\parallel$ and $m_2^\parallel$ are both positive). Note that, since $\vec{m}_1$ and $\vec{m}_2$ are not assumed to be orthogonal, conditions (2.5a) and (2.5b) are not redundant.

2.2 Perspective 1: the 1D quasilattice from dualizing a 1D bi-grid

The $\{\vec{m}_1, \vec{m}_2\}$ basis defines an "integer grid": this is the set of all lines that (in the $\{\vec{m}_1, \vec{m}_2\}$ basis) have a constant integer value for either their first or second coordinate (like the grid of lines on an ordinary sheet of graph paper). The intersection of this integer grid with the line $\vec{q}(t)$ defines a natural 1D "bi-grid." In particular, the grid line whose first coordinate

(in the $\{\vec{m}_1, \vec{m}_2\}$ basis) is the integer $n \in \mathbb{Z}$ intersects $\vec{q}(t)$ at $t = t_n^{(1)}$, where

$$\widetilde{m}^1 \vec{q}(t_n^{(1)}) = n \qquad \Rightarrow \qquad t_n^{(1)} = \frac{n - \widetilde{m}^1 \vec{q}_0}{\widetilde{m}^1 \hat{e}_\parallel}, \tag{2.6a}$$

while the grid line whose second coordinate (in the $\{\vec{m}_1, \vec{m}_2\}$ basis) is the integer $n \in \mathbb{Z}$ intersects $\vec{q}(t)$ at $t = t_n^{(2)}$, where

$$\widetilde{m}^2 \vec{q}(t_n^{(2)}) = n \qquad \Rightarrow \qquad t_n^{(2)} = \frac{n - \widetilde{m}^2 \vec{q}_0}{\widetilde{m}^2 \hat{e}_\parallel}. \tag{2.6b}$$

The points $t_n^{(1)}$ form a periodic 1D lattice of spacing $1/(\widetilde{m}^1 \hat{e}_\parallel)$, while the points $t_n^{(2)}$ form another periodic 1D lattice of spacing $1/(\widetilde{m}^2 \hat{e}_\parallel)$. The superposition of these two periodic lattices (with incommensurate spacings) is the 1D bi-grid.

From this 1D bi-grid, we obtain the corresponding 1D quasilattice by a standard "dualization" procedure []: to each space between two consecutive points in the bi-grid, we assign a point x in the dual quasilattice, so that (i) whenever we cross a point $t_n^{(1)}$ in the bi-grid (from the $t_{n-1}^{(1)}$ side to the $t_{n+1}^{(1)}$ side), we correspondingly jump $x \to x + m_1^\parallel$ in the dual quasi-lattice, and (ii) whenever we cross a point $t_n^{(2)}$ in the bi-grid (from the $t_{n-1}^{(2)}$ side to the $t_{n+1}^{(2)}$ side), we correspondingly jump $x \to x + m_2^\parallel$ in the dual quasi-lattice. Stated another way, as the bi-grid parameter t continuously sweeps from $-\infty$ to $+\infty$, the quasilattice point x changes discretely, according to the formula

$$x = \left\lfloor \widetilde{m}^1 \vec{q}(t) \right\rfloor m_1^\parallel + \left\lfloor \widetilde{m}^2 \vec{q}(t) \right\rfloor m_2^\parallel + C \tag{2.7}$$

where C is a constant.

We can canonically fix C by demanding that the quasilattice dual to a reflection-symmetric bi-grid is also reflection-symmetric, which fixes C to be:

$$C = \frac{1}{2} m_1^\parallel + \frac{1}{2} m_2^\parallel - q_0^\parallel. \tag{2.8}$$

Fixing this phase relationship is unimportant in 1D, but plays an important role when we construct higher-dimensional Ammann patterns in [12], since these higher-dimensional Ammann patterns are built from a collection of multiple 1D quasilattices whose phases must be carefully coordinated with one another.

2.3 Perspective 2: the 1D quasilattice from a cut-and-project algorithm

Eqs. (2.7) and (2.8) also have another geometric interpretation. We can think of the $\{\vec{m}_1, \vec{m}_2\}$ integer grid described in Subsection 2.2 as slicing up the plane into parallelograms whose edges are the vectors $\vec{m}_1$ and $\vec{m}_2$, and whose vertices coincide with the points of Λ. Now we can construct our 1D quasilattice by the following "cut-and-project" algorithm: whenever the "cut" line $\vec{q}(t)$ intersects one of these parallelograms, we orthogonally project the midpoint of that parallelogram onto the cut line to obtain the point $\vec{q}(x)$ (see Fig. 1). This mapping from t to x is precisely the one described by Eqs. (2.7) and (2.8).

In particular, fixing C according to (2.8) corresponds to projecting the parallelogram's midpoint.

This cut-and-project perspective leads to a convenient way of re-expressing Eqs. (2.7) and (2.8). For the rest of this section, let us assume that $\{\vec{m}_1, \vec{m}_2\}$ are a *positive* basis (see Subsection 2.1). As t runs from $-\infty$ to $+\infty$, the line $\vec{q}(t)$ passes from one parallelogram to the next, thereby placing the parallelograms that it intersects in a specific order, which can be indexed by the integer n. In particular, when $\vec{q}(t)$ passes through the nth parallelogram, it intersects that parallelogram's transverse diagonal at a time t_n given by:

$$\widetilde{m}\,\vec{q}(t_n) = n \qquad \Rightarrow \qquad t_n = \frac{n - \widetilde{m}\,\vec{q}_0}{\widetilde{m}\hat{e}_\parallel} \tag{2.9}$$

where

$$\widetilde{m} = \widetilde{m}^1 + \widetilde{m}^2. \tag{2.10}$$

We can use Eqs. (2.7) and (2.8) to map this nth intersection time, t_n, to a corresponding nth point in the quasilattice, x_n. Following this procedure and massaging the result a bit, we obtain the useful formula:

$$x_n = \left(\left\lfloor \frac{nm_2^\perp - q_0^\perp}{m_2^\perp - m_1^\perp} \right\rfloor + \frac{1}{2} \right) m_1^\parallel + \left(\left\lfloor \frac{nm_1^\perp - q_0^\perp}{m_1^\perp - m_2^\perp} \right\rfloor + \frac{1}{2} \right) m_2^\parallel - q_0^\parallel. \tag{2.11}$$

Let us make three remarks about Eq. (2.11):

1. Eq. (2.11) defines the same 1D quasilattice as Eqs. (2.7, 2.8); the difference is that, whereas Eqs. (2.7, 2.8) expressed this quasilattice as the range of a many-to-one map with a continuous domain ($t \in \mathbb{R}$), Eq. (2.11) expresses the same quasilattice as the range of a one-to-one map from a discrete domain ($n \in \mathbb{Z}$).

2. Imagine replacing the line $\vec{q} = \vec{q}_0 + \hat{e}_\parallel t$ by a new line $\vec{q}\,' = \vec{q}_0\,' + \hat{e}_\parallel t$ which is parallel to the original line, and has just been translated by a vector in Λ: $\vec{q}_0\,' = \vec{q}_0 + n_1\vec{m}_1 + n_2\vec{m}_2$ (for some integers n_1 and n_2). Then, via Eq. (2.11), we obtain a new quasilattice x_n' with correspondingly shifted parameters:

$$\begin{aligned} q_0^{\parallel\,\prime} &= q_0^\parallel + n_1 m_1^\parallel + n_2 m_2^\parallel, \\ q_0^{\perp\,\prime} &= q_0^\perp + n_1 m_1^\perp + n_2 m_2^\perp. \end{aligned} \tag{2.12}$$

But, as may be checked from Eq. (2.11), the two quasilattices x_n and x_n' are actually identical up to reindexing: $x_n' = x_{n-n_1-n_2}$. This is called an *umklaap transformation* [21] and reflects the fact that, when we consider the family of 1D quasilattices obtained by varying $\vec{q}_0$, we can really think of $\vec{q}_0$ as living on a torus [22, 23].

3. Since $\{\vec{m}_1, \vec{m}_2\}$ is a positive basis, Eq. (2.5a) requires $m_2^\perp/m_1^\perp < 0$, and Eq. (2.5b) requires $m_1^\parallel > 0$ and $m_2^\parallel > 0$. Together these conditions imply that, as the integer index n increments (from n' to $n'+1$), the corresponding quasilattice position x_n (2.11) increases by one of the two positive lengths: $m_1^\parallel$ or $m_2^\parallel$. Furthermore,

$$(f_1/f_2) = -(m_2^\perp/m_1^\perp), \tag{2.13}$$

where f_1/f_2 is the relative frequency of steps of length $m_1^{\parallel}$ and steps of length $m_2^{\parallel}$. If $f_1/f_2 < 1$, the quasilattice consists of single (isolated) steps of length $m_1^{\parallel}$, separated by either $\lfloor f_2/f_1 \rfloor$ or $(\lfloor f_2/f_1 \rfloor + 1)$ steps of length $m_2^{\parallel}$; and if $f_2/f_1 < 1$, the quasi-lattice consists of single (isolated) steps of length $m_2^{\parallel}$, separated by either $\lfloor f_1/f_2 \rfloor$ or $(\lfloor f_1/f_2 \rfloor + 1)$ steps of length $m_1^{\parallel}$.

Although Eq. (2.11) has the advantage of being manifestly symmetric under interchange of $1 \leftrightarrow 2$ subscripts, it is sometimes convenient to rewrite it in one of the following two forms, which each only involve one floor function $\lfloor \ldots \rfloor$, and are swapped by swapping $1 \leftrightarrow 2$:

$$x_n = m_1^{\parallel}(n - \chi_1^{\parallel}) + (m_2^{\parallel} - m_1^{\parallel}) \left(\left\lfloor \kappa_1(n - \chi_1^{\perp}) \right\rfloor + \frac{1}{2} \right) \tag{2.14a}$$

$$= m_2^{\parallel}(n - \chi_2^{\parallel}) + (m_1^{\parallel} - m_2^{\parallel}) \left(\left\lfloor \kappa_2(n - \chi_2^{\perp}) \right\rfloor + \frac{1}{2} \right) \tag{2.14b}$$

where we have defined the constants

$$\chi_1^{\parallel} \equiv q_0^{\parallel}/m_1^{\parallel}, \qquad \chi_1^{\perp} \equiv q_0^{\perp}/m_1^{\perp}, \qquad \kappa_1 \equiv \frac{m_1^{\perp}}{m_1^{\perp} - m_2^{\perp}}, \tag{2.15a}$$

$$\chi_2^{\parallel} \equiv q_0^{\parallel}/m_2^{\parallel}, \qquad \chi_2^{\perp} \equiv q_0^{\perp}/m_2^{\perp}, \qquad \kappa_2 \equiv \frac{m_2^{\perp}}{m_2^{\perp} - m_1^{\perp}}. \tag{2.15b}$$

Let us add three more remarks:

1. When we re-express the quasilattice (2.11) in the form (2.14), we correspondingly re-express the umklaap transformation (2.12) in the form

$$\chi_1^{\parallel\prime} = \chi_1^{\parallel} + n_1 + n_2(m_2^{\parallel}/m_1^{\parallel}), \qquad \chi_1^{\perp\prime} = \chi_1^{\perp} + n_1 + n_2(m_2^{\perp}/m_1^{\perp}), \quad \text{(2.16a)}$$
$$\chi_2^{\parallel\prime} = \chi_2^{\parallel} + n_2 + n_1(m_1^{\parallel}/m_2^{\parallel}), \qquad \chi_2^{\perp\prime} = \chi_2^{\perp} + n_2 + n_1(m_1^{\perp}/m_2^{\perp}). \quad \text{(2.16b)}$$

2. In the generic (non-singular) case where the line $\vec{q}(t)$ does not intersect any of the points in Λ, the three expressions (2.11, 2.14a, 2.14b) are all equivalent. In the special (singular) case where the line $\vec{q}(t)$ intersects a point in Λ, the three expressions (2.11, 2.14a, 2.14b) are *almost* equivalent, but they differ at one point x_{n_*} (where the argument of the floor function $\lfloor \ldots \rfloor$ is precisely an integer). This may seem like a minor detail, but in fact (as we shall explain in a subsequent paper [20]) these special cases are not only the 1D analogues of, but also the 1D building blocks for, a fascinating set of topological defects which are intrinsic to two- and higher-dimensional Penrose-like tilings (and are known as "decapod defects" in the case of the standard 2D Penrose tiling [2, 5]). For this reason, we will continue to keep track of this detail at later points in this paper (see Section 4 and Appendix B).

3. Comparing Eqs. (2.1) and (2.14), we see that *given a line $\vec{q}(t)$, a lattice Λ, and a positive basis $\{\vec{m}_1, \vec{m}_2\}$, the cut-and-project algorithm described above produces a quadratic 1D quasilattice x_n.* Conversely, it is easy to check that *any quadratic 1D*

quasilattice x_n may be obtained from such a cut-and-project algorithm: the "‖" components of $\vec{m}_1$ and $\vec{m}_2$ can be chosen to obtain the desired parameters S and L, the "⊥" components of $\vec{m}_1$ and $\vec{m}_2$ can be chosen to obtain the desired κ, and the "‖" and "⊥" components of $\vec{q}_0$ can be chosen to obtain the desired $\{\alpha, \beta\}$.

2.4 Perspective 3: the 1D quasilattice from slicing a 2-torus

The lattice Λ defines a 2-torus (obtained by identifying the opposite edges of the $\{\vec{m}_1, \vec{m}_2\}$ parallelogram described above). Then $\vec{q}(t)$ is a geodesic with irrational slope that wraps around and around the torus forever, densely covering its surface without ever intersecting itself. The midpoints of the $\{\vec{m}_1, \vec{m}_2\}$ parallelograms are mapped to a single marked point P on the torus. Now, let us imagine drawing a second geodesic segment on the torus: perpendicular to $\vec{q}(t)$, of length $|m_2^\perp - m_1^\perp|$, and centered on the point P. This segment intersects the original geodesic $\vec{q}(x)$ at an infinite number of points, and the intersection times are precisely the quasilattice positions x_n described by Eqs. (2.7, 2.8) or, equivalently, by Eqs. (2.11) or (2.14).

3 Lattice-equivalent quasilattices

In Section 2, we constructed the quadratic 1D quasilattice x_n (2.11) by first choosing: (i) a line $\vec{q}(t)$, (ii) a lattice Λ, and (iii) a "positive" integer basis $\{\vec{m}_1, \vec{m}_2\}$ for Λ. If, instead, we had chosen the *same* line $\vec{q}(t)$ and the *same* lattice Λ, but a *different* positive integer basis $\{\vec{m}_1', \vec{m}_2'\}$, we would have obtained a different quadratic quasilattice:

$$x_n' = \left(\left\lfloor \frac{nm_2^{\perp\prime} - q_0^\perp}{m_2^{\perp\prime} - m_1^{\perp\prime}} \right\rfloor + \frac{1}{2} \right) m_1^{\|\prime} + \left(\left\lfloor \frac{nm_1^{\perp\prime} - q_0^\perp}{m_1^{\perp\prime} - m_2^{\perp\prime}} \right\rfloor + \frac{1}{2} \right) m_2^{\|\prime} - q_0^\|. \qquad (3.1)$$

We will call two quasilattices x_n and x_n' that are related in this way "lattice equivalent."

To understand lattice equivalence in more detail, let us write the relationship between the two bases as

$$\vec{m}_1' = a\vec{m}_1 + b\vec{m}_2, \qquad (3.2a)$$

$$\vec{m}_2' = c\vec{m}_1 + d\vec{m}_2. \qquad (3.2b)$$

Since $\{\vec{m}_1, \vec{m}_2\}$ and $\{\vec{m}_1', \vec{m}_2'\}$ are both integer bases for Λ,

$$\tau = \begin{pmatrix} a & b \\ c & d \end{pmatrix} \qquad (3.3)$$

must be an integer matrix with determinant ± 1. And since $\{\vec{m}_1, \vec{m}_2\}$ and $\{\vec{m}_1', \vec{m}_2'\}$ are both *positive* integer bases for Λ and, without loss of generality, we take the unprimed $\{\vec{m}_1, \vec{m}_2\}$ parallelogram to be the one that is wider in the $\hat{e}_\perp$ direction ($|m_2^\perp - m_1^\perp| > |m_2^{\perp\prime} - m_1^{\perp\prime}|$), the components $\{a, b, c, d\}$ of τ must also all be non-negative (see Appendix A for a proof).

The two lattice-equivalent quasilattices x_n (2.11) and x_n' (3.1) are intimately related to one another: the denser quasilattice x_n may be obtained from the sparser quasilattice x_n' by applying a local "substitution" or "decoration" rule that replaces each type of interval
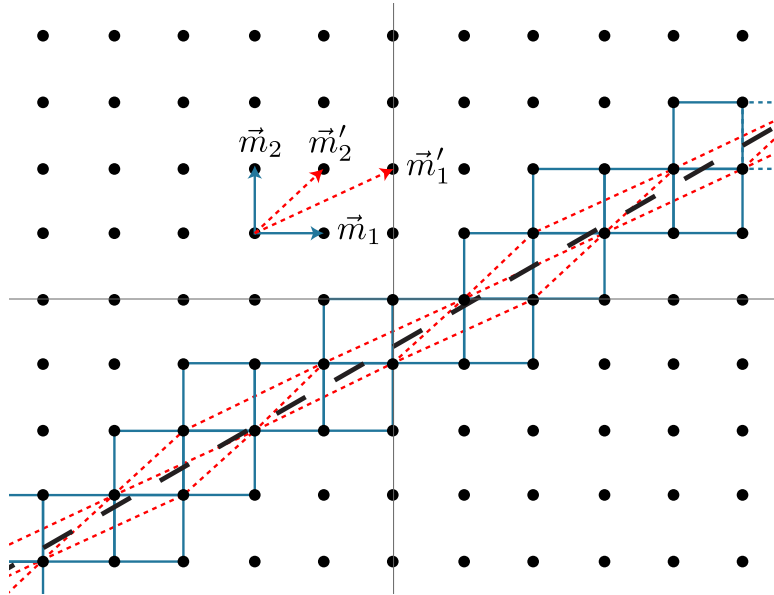
Figure 3. Illustrates why two lattice equivalent quasilattices are related by a fixed decoration rule, as explained in Section 3.

between points in the sparser quasilattice by a specific, fixed sequence of intervals in the denser quasilattice; and in the other direction, the sparser quasilattice may be recovered from the denser one by a local rule for gluing together a certain specific, fixed sequence of intervals in the denser lattice to obtain each type of interval in the sparser one.

To understand this assertion, consider Fig. 3: it shows the set of (red, elongated, dotted) $\{\vec{m}_1', \vec{m}_2'\}$ parallelograms and the set of (blue, square, solid) $\{\vec{m}_1, \vec{m}_2\}$ parallelograms that are intersected by the diagonal black dotted line $\vec{q}(t)$. Note that the set of $\{\vec{m}_1, \vec{m}_2\}$ parallelograms is precisely the minimal set needed to cover the set of $\{\vec{m}_1', \vec{m}_2'\}$ parallelograms completely. (For clarity, in the top panel of Fig. 4 we show a single $\{\vec{m}_1', \vec{m}_2'\}$ parallelogram and its minimal covering by $\{\vec{m}_1, \vec{m}_2\}$ parallelograms; and in the bottom panel of Fig. 4, we show the minimal covering of two adjacent $\{\vec{m}_1', \vec{m}_2'\}$ parallelograms, depending on whether they share a common long edge or a common short edge.) From Figs. 3 and 4, we can see the simple geometric reason why (as asserted above) the denser quasilattice x_n may be obtained from the sparser quasilattice x_n' by applying a fixed "substitution" or "decoration" rule to each of the two intervals (S' and L') in the x_n' quasilattice – it is because: (i) whenever two adjacent $\{\vec{m}_1', \vec{m}_2'\}$ parallelograms share a common *short* edge (giving rise to an L' interval in this example), they are always covered by the same arrangement of $\{\vec{m}_1, \vec{m}_2\}$ parallelograms, which yields a fixed decoration of L' by S and L; and (ii) similarly, whenever two adjacent $\{\vec{m}_1', \vec{m}_2'\}$ parallelograms share a common *long* edge (giving rise to an S' interval in this example), they are always covered by the same arrangement of $\{\vec{m}_1, \vec{m}_2\}$ parallelograms, which yields a fixed decoration of S' by S and L.

Lattice equivalence thus organizes the various quadratic 1D quasilattices x_n obtained the previous section into lattice equivalence classes (with an uncountable infinity of different
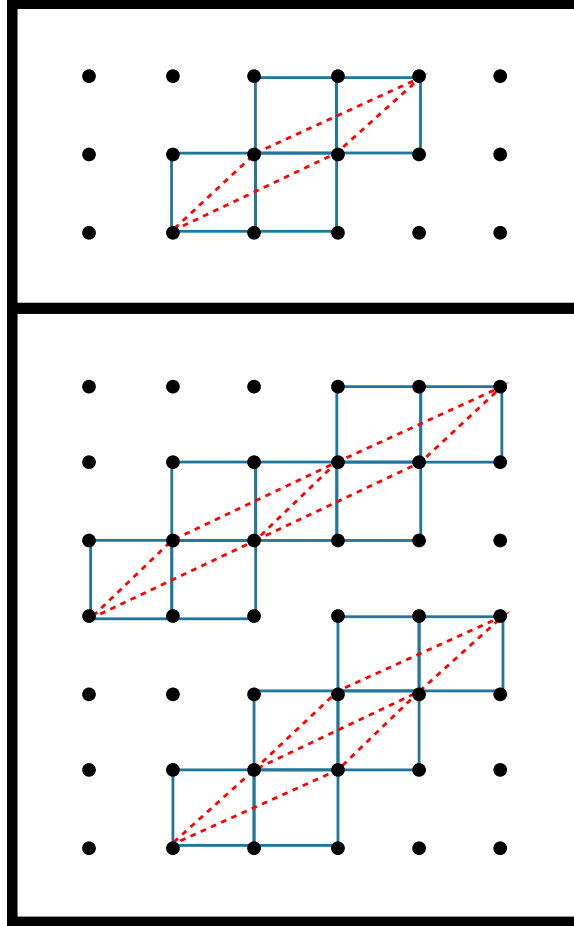
Figure 4. More about the relationship between the parallelograms in Fig. 3: the top panel shows the minimal covering of one (red, elongated, dotted) $\{\vec{m}'_1, \vec{m}'_2\}$ parallelogram by (blue, square, solid) $\{\vec{m}_1, \vec{m}_2\}$ parallelograms; and the bottom panel shows the minimal covering of two adjacent $\{\vec{m}'_1, \vec{m}'_2\}$, which just depends on whether they share a common short edge, or a common long edge.

lattice equivalence classes, and a countable infinity of different quasilattices in any particular lattice equivalence class). Given a fixed line $\vec{q}(t)$ and a fixed lattice Λ, the various members of the corresponding lattice equivalence class come from all the different ways of choosing a positive integer basis $\{\vec{m}_1, \vec{m}_2\}$ for Λ; and any two members of the family may be derived from one another by a local substitution/gluing rule corresponding to the integer matrix τ.

The notion of lattice equivalence elucidates the precise connection between substitution sequences, on the one hand, and cut-and-project sequences, on the other. On the one hand, if the quasilattices x_n and x'_n are lattice equivalent, the sequence x_n (regarded as an infinite string of unprimed letters S and L) may be algebraically obtained from the sequence x'_n (regarded as an infinite string of primed letters S' and L') by a formal substitution rule in which each primed letter (S' or L') is replaced by a fixed finite string of unprimed letters (S and L). This substitution rule may be summarized by a 2×2 integer matrix τ in a standard way. On the other hand, we see that this *same* matrix τ has a simple geometric meaning:

it is precisely the matrix that connects the unprimed basis $\{\vec{m}_1, \vec{m}_2\}$ (that produces x_n via cut-and-project) to the primed basis $\{\vec{m}_1', \vec{m}_2'\}$ (that produces x_n' via cut-and-project).

Furthermore, from the algebraic perspective, the matrix τ is not enough to specify the substitution rule, since it doesn't fix the particular ordering or overall translational phase of the substitution rule. For example, the matrix

$$\tau = \begin{pmatrix} 1 & 1 \\ 2 & 3 \end{pmatrix} \tag{3.4}$$

might correspond to any of the following three substitution rules:

$$\{S', L'\} \to \{\frac{L}{2}S\frac{L}{2}, \frac{L}{2}SLLS\frac{L}{2}\} \tag{3.5a}$$

$$\{S', L'\} \to \{\frac{L}{2}S\frac{L}{2}, \frac{L}{2}LSSL\frac{L}{2}\} \tag{3.5b}$$

$$\{S', L'\} \to \{SL, SLLSL\}. \tag{3.5c}$$

Note that, (3.5a) and (3.5b) correspond to different orderings, while (3.5a) and (3.5c) correspond to different phases – *i.e.* if we start from the same parent sequence and apply these substitutions, then (3.5a) and (3.5b) will produce two genuinely distinct daughter sequences, while (3.5a) and (3.5c) will produce two sequences that only differ by an overall translation by $L/2$. By contrast, from the geometrical perspective, the matrix τ *also* determines an ordering and a phase – *i.e.* it is associated with a canonical substitution rule and, in particular, one that is $x \to -x$ reflection symmetric. For example, for τ given by Eq. (3.4), the canonical substitution rule is given by (3.5a) – see Row 3b in Table 1. These canonical substitution rules (including ordering and phase) will be important in our analysis of higher-dimensional Ammann patterns in [12].

4 Self-similar quasilattices

Two 1D quasilattices are locally isomorphic if any finite segment which occurs in one quasilattice also occurs somewhere in the other quasilattice, and vice versa, so that it is impossible, by inspecting any finite segment, to determine which of the two quasilattices one is looking at (see *e.g.* [2, 10, 21] for more). Two lattice-equivalent quasilattices x_n and x_n', related by the matrix τ, may look very different from one another and, in general, will not be locally isomorphic, even after an overall rescaling. If x_n and x_n' are *also* locally isomophic (up to overall rescaling), then we say they are *self-similar* (under the transformation τ). In this section, we give the general closed-form expression for a self-similar quadratic 1D quasilattice, and a simple rule for how its parameters transform under a self-similarity (inflation/deflation) transformation. Then, in Table 1, we collect the ten special self-similar sequences that are relevant for constructing higher-dimensional Ammann patterns [12]; and in Figure 5, we depict the corresponding substitution rules.

To start, let us pick a particular transformation matrix

$$\tau = \begin{pmatrix} a & b \\ c & d \end{pmatrix} \tag{4.1}$$

(with non-negative integer components and determinant ± 1). In the self-similar case, the new quasilattice x'_n (3.1) is related to the original one x_n (2.11) by

$$\frac{m_1^{\|'}}{m_2^{\|'}} = \frac{m_1^{\|}}{m_2^{\|}} \qquad \text{and} \qquad \frac{m_1^{\perp'}}{m_2^{\perp'}} = \frac{m_1^{\perp}}{m_2^{\perp}}; \tag{4.2}$$

or, equivalently,

$$\begin{pmatrix} m_1^{\|} \\ m_2^{\|} \end{pmatrix} \qquad \text{and} \qquad \begin{pmatrix} m_1^{\perp} \\ m_2^{\perp} \end{pmatrix} \tag{4.3}$$

must be two *different* eigenvectors of τ with corresponding eigenvalues

$$\lambda_{\|} = \frac{1}{2}\left[a + d + \sqrt{(a+d)^2 - 4(ad - bc)}\right] \tag{4.4a}$$

$$\lambda_{\perp} = \frac{1}{2}\left[a + d - \sqrt{(a+d)^2 - 4(ad - bc)}\right] \tag{4.4b}$$

where $\lambda_{\|} > 1$, while $|\lambda_{\perp}| < 1$ and $\text{sign}(\lambda_{\perp}) = \det(\tau)$.

If the quasilattice x_n (2.11, 2.14a, 2.14b) is self-similar with respect to the transformation τ, then after s successive transformations, the resulting sequence $x_{n,s}$ is:

$$\frac{x_{n,s}}{\lambda_{\|}^s} = \left(\left\lfloor \frac{nm_2^{\perp} - q_{0,s}^{\perp}}{m_2^{\perp} - m_1^{\perp}} \right\rfloor + \frac{1}{2}\right) m_1^{\|} + \left(\left\lfloor \frac{nm_1^{\perp} - q_{0,s}^{\perp}}{m_1^{\perp} - m_2^{\perp}} \right\rfloor + \frac{1}{2}\right) m_2^{\|} - q_{0,s}^{\|} \tag{4.5a}$$

$$= m_1^{\|}(n - \chi_{1,s}^{\|}) + (m_2^{\|} - m_1^{\|})\left(\left\lfloor \kappa_1(n - \chi_{1,s}^{\perp}) \right\rfloor + \frac{1}{2}\right) \tag{4.5b}$$

$$= m_2^{\|}(n - \chi_{2,s}^{\|}) + (m_1^{\|} - m_2^{\|})\left(\left\lfloor \kappa_2(n - \chi_{2,s}^{\perp}) \right\rfloor + \frac{1}{2}\right) \tag{4.5c}$$

with new parameters $\{q_{0,s}^{\|}, q_{0,s}^{\perp}\}$ (or $\{\chi_{1,s}^{\|}, \chi_{1,s}^{\perp}\}$ or $\{\chi_{2,s}^{\|}, \chi_{2,s}^{\perp}\}$) which are related to the original parameters $\{q_0^{\|}, q_0^{\perp}\}$ (or $\{\chi_1^{\|}, \chi_1^{\perp}\}$ or $\{\chi_2^{\|}, \chi_2^{\perp}\}$) as follows

$$q_{0,s}^{\|} \equiv \frac{q_0^{\|}}{\lambda_{\|}^s}, \qquad q_{0,s}^{\perp} \equiv \frac{q_0^{\perp}}{\lambda_{\perp}^s}, \tag{4.6a}$$

$$\chi_{1,s}^{\|} \equiv \frac{\chi_1^{\|}}{\lambda_{\|}^s}, \qquad \chi_{1,s}^{\perp} \equiv \frac{\chi_1^{\perp}}{\lambda_{\perp}^s}, \tag{4.6b}$$

$$\chi_{2,s}^{\|} \equiv \frac{\chi_2^{\|}}{\lambda_{\|}^s}, \qquad \chi_{2,s}^{\perp} \equiv \frac{\chi_2^{\perp}}{\lambda_{\perp}^s}. \tag{4.6c}$$

More precisely, Eqs. (4.5) and (4.6) are correct in the generic (non-singular) case where $\vec{q}(t)$ doesn't intersect any points in Λ; and in the special (singular) case where $\vec{q}(t)$ intersects one point in Λ they are *almost* correct – *i.e.* they are correct everywhere except at the one (singular) point in the quasilattice where the argument of the floor function $\lfloor \ldots \rfloor$ is equal to an integer. As mentioned in Section 2, this apparently minor detail is important because (as we shall see in a subsequent paper [20]) these special 1D quasilattices play an important role in describing and understanding the intrinsic "topological" defects which can arise

Case	$\lambda_\pm$	τ	$m_2^\pm/m_1^\pm$	S'	L'
1	$\frac{1}{2}(1\pm\sqrt{5})$	$\begin{pmatrix} 0 & 1 \\ 1 & 1 \end{pmatrix}$	$\frac{1}{2}(1\pm\sqrt{5})$	$\frac{L}{2}\frac{L}{2}$	$\frac{L}{2}S\frac{L}{2}$
2a	$1\pm\sqrt{2}$	$\begin{pmatrix} 1 & 1 \\ 2 & 1 \end{pmatrix}$	$\pm\sqrt{2}$	$\frac{L}{2}S\frac{L}{2}$	$\frac{L}{2}SS\frac{L}{2}$
2b	$1\pm\sqrt{2}$	$\begin{pmatrix} 0 & 1 \\ 1 & 2 \end{pmatrix}$	$1\pm\sqrt{2}$	L	LSL
3a	$2\pm\sqrt{3}$	$\begin{pmatrix} 1 & 2 \\ 1 & 3 \end{pmatrix}$	$\frac{1}{2}(1\pm\sqrt{3})$	$\frac{S}{2}LL\frac{S}{2}$	$\frac{S}{2}LLL\frac{S}{2}$
3b	$2\pm\sqrt{3}$	$\begin{pmatrix} 2 & 1 \\ 3 & 2 \end{pmatrix}$	$\pm\sqrt{3}$	SLS	$SLSLS$
3c	$2\pm\sqrt{3}$	$\begin{pmatrix} 1 & 1 \\ 2 & 3 \end{pmatrix}$	$1\pm\sqrt{3}$	$\frac{L}{2}S\frac{L}{2}$	$\frac{L}{2}SLLS\frac{L}{2}$
4a	$2\pm\sqrt{5}$	$\begin{pmatrix} 3 & 1 \\ 4 & 1 \end{pmatrix}$	$-1\pm\sqrt{5}$	$\frac{L}{2}SSS\frac{L}{2}$	$\frac{L}{2}SSSS\frac{L}{2}$
4b	$2\pm\sqrt{5}$	$\begin{pmatrix} 2 & 1 \\ 5 & 2 \end{pmatrix}$	$0\pm\sqrt{5}$	SLS	$SLSSSLS$
4c	$2\pm\sqrt{5}$	$\begin{pmatrix} 1 & 1 \\ 4 & 3 \end{pmatrix}$	$1\pm\sqrt{5}$	$\frac{L}{2}S\frac{L}{2}$	$\frac{L}{2}SLSSLS\frac{L}{2}$
4d	$2\pm\sqrt{5}$	$\begin{pmatrix} 0 & 1 \\ 1 & 4 \end{pmatrix}$	$2\pm\sqrt{5}$	L	$LLSLL$

Table 1. Catalog of the ten 1D self-similar quasilattices relevant to constructing higher-dimensional Ammann patterns and Penrose-like tilings in [12]. In this table, we use the convenient notation $\lambda_\pm$ and $m_i^\pm$ where here the superscript/subscript "+" stands for the former subscript/superscript "$\parallel$", while the "$-$" stands for "$\perp$". Within each case, the subcases are in order of increasing L/S.

in Penrose-like tilings in two and higher dimensions (like the so-called "decapod" defects in the ordinary Penrose tiling [2, 5]). If we want to describe 1D quasilattices and their self-similarity transformations in a way that continues to be precisely correct, even in the singular case, we have to replace Eqs. (4.5a, 4.5b, 4.5c) by the corresponding Eqs. (4.5a′, 4.5b′, 4.5c′) presented in Appendix B.

In our subsequent paper [12], where these self-similar 1D quasilattices are used as the building blocks for higher dimensional Ammann patterns and Penrose-like tilings, four cases are relevant (see Table 1 in [24]): Case 1, where the scaling factor is the "golden ratio", $\lambda_\parallel = \phi = (1 + \sqrt{5})/2$, which is the relevant case for describing systems with 5-fold or 10-fold order in 2D, some systems with icosahedral (H_3) order in 3D, and systems with "hyper-icosahedral" (H_4) order in 4D; Case 2, where the scale factor is the "silver ratio" $\lambda_\parallel = (1+\sqrt{2})$, which is the relevant case for describing systems with 8-fold order in 2D; Case 3, where the scale factor is $\lambda_\parallel = (2 + \sqrt{3})$, which is the relevant case for describing systems

Figure 5. Illustrations of the ten 1D self-similar substitution rules relevant to constructing higher-dimensional Ammann patterns and Penrose-like tilings (as catalogued in the last column of Table 1). In each row of this figure, the short (solid, purple) and long (dashed, turqoise) prototiles are on the bottom, with their corresponding self-similar decimations into smaller tiles directly above. Open circles indicate the endpoints of tiles. Complete tiles have have circles at both ends; half tiles have a circle at one end but none at the half-way point. For example, Row 1 shows how a short prototile S' (bottom left) is subdivided into two halves of a long prototile: $S' = (L/2)(L/2)$ (top left); and a long prototile L' (bottom right) is subdivided into $L' = (L/2)S(L/2)$ (top right).

with 12-fold order in 2D; and Case 4, where the scale factor is $\lambda_\parallel = \phi^3 = 2 + \sqrt{5}$, which is the relevant case for describing some systems with icosahedral (H_3) order in 3D. In Table 1 we list all ten of the 1D self-similar quasilattices corresponding to these four cases, and provide the relevant parameters needed to describe them explicitly.[1] Note that in this table we have used the convenient notation $\lambda_\pm$ and $m_i^\pm$ where here the "+" superscript/subscript stands for the former superscript/subscript "$\parallel$", and similarly the "$-$" stands for "$\perp$".

5 Self-same quasilattices

In the previous section, we restricted our attention to 1D quasilattices that were *self-similar* (*i.e.* both lattice equivalent and locally isomorphic) under the transformation τ. In this section, we restrict our attention further to 1D quasilattices x_n that are *s-fold self-same* with respect to τ – meaning that x_n is self-similar with respect to τ and, moreover, $x_{n,s}$ (the quasilattice obtained by performing s successive τ-transformations) is *identical* to x_n (after an appropriate rescaling).

In the previous section, we found that after s successive τ transformations, the original quasilattice x_n (2.11, 2.14a, 2.14b) characterized by parameters $\{q_0^\parallel, q_0^\perp\}$ (or $\{\chi_1^\parallel, \chi_1^\perp\}$ or $\{\chi_2^\parallel, \chi_2^\perp\}$) was transformed to a new quasilattice $x_{n,s}$ (4.5a, 4.5b, 4.5c) characterized by new parameters $\{q_{0,s}^\parallel, q_{0,s}^\perp\}$ (or $\{\chi_{1,s}^\parallel, \chi_{1,s}^\perp\}$ or $\{\chi_{2,s}^\parallel, \chi_{2,s}^\perp\}$). In order for x_n to be s-fold self-same, these transformed parameters must be related to the original parameters by an umklaap transformation (2.12, 2.16a, 2.16b). This implies that a quasilattice will be s-fold self-same with respect to τ if it is self-similar with respect to τ and, in addition, its parameters are given by

$$q_0^\pm = \frac{\lambda_\pm^s(n_1 m_1^\pm + n_2 m_2^\pm)}{1 - \lambda_\pm^s}, \tag{5.1a}$$

$$\chi_1^\pm = \frac{\lambda_\pm^s(n_1 m_1^\pm + n_2 m_2^\pm)}{(1 - \lambda_\pm^s)m_1^\pm}, \tag{5.1b}$$

$$\chi_2^\pm = \frac{\lambda_\pm^s(n_2 m_2^\pm + n_1 m_1^\pm)}{(1 - \lambda_\pm^s)m_2^\pm}, \tag{5.1c}$$

for any integers n_1 and n_2 (where, again in this section, we are using the notation that superscripts/subscripts + and $-$ stand for $\parallel$ and $\perp$, respectively).

As it stands, this answer is redundant, because there can be different ordered pairs $\{n_1, n_2\}$ and $\{n_1', n_2'\}$ of integers for which the above parameters secretly describe the same quasilattice (up to umklaap). In order to count the non-redundant self-same crystals, first

---

[1]Note that some of these were already fully or partially described in the literature, and others seem not to have been. Case 1 (the Fibonacci lattice) and its canonical substitution rule were known in one form or another at least since Ammann came across them in the 1970's, and an early instance of its explicit floor-form expression and the corresponding canonical inflation/deflation rule may be found in [21]. Case 2a was the subject of [13] and is also in [25], along with Case 3a. In addition, all three of the 2×2 transformation matrices corresponding to the ratio $(2 + \sqrt{3})$ may be found in [10] (but not the corresponding closed-form expressions for the quasilattice and its self-similarity transformation, or the canonical substitution rule, including ordering and phase).

note that matrix τ has eigenvalues

$$\lambda_\pm = \frac{1}{2}[(a+d) \pm \sqrt{(a+d)^2 - 4\det(\tau)}] \tag{5.2}$$

which satisfy

$$\lambda_\pm^s = F_s \lambda_\pm - F_{s-1}\det(\tau) \tag{5.3}$$

where the coefficients F_s are determined by the recursion relation

$$F_{s+1} = (a+d)F_s - \det(\tau)F_{s-1}, \tag{5.4}$$

with initial conditions $F_0 = 0$ and $F_1 = 1$. Next note that, from (5.3) together with the fact that $\lambda_+\lambda_- = \det(\tau)$, we obtain the useful identities

$$(1 - \lambda_+^s)(1 - \lambda_-^s) = 1 + \det(\tau)F_{s-1} - F_{s+1} + (\det \tau)^s \tag{5.5}$$

and

$$(\det \tau)^{s-1} = F_s^2 - F_{s-1}F_{s+2}. \tag{5.6}$$

Putting these results together, we find that the number of quasilattices that are s-fold self-same with respect to τ is given by

$$N_s = F_{s+1} - \det(\tau)F_{s-1} - \frac{3 + \det(\tau)}{2}. \tag{5.7}$$

But this result is not yet what we want, since it includes quasilattices that are self-same after s inflations, but were already self same after r inflations, where r is a divisor of s. After we remove these "reducible" cases, we are left with the number $\langle N_s \rangle$ of *irreducible* s-fold self-same quasilattices. The number $\langle N_s \rangle$ is divisible by s, since the irreducible s-fold self-same quasilattices are grouped into families of size s which cycle into one another under τ-transformation, and which we will call "s-cycles." So the most natural thing to count is the number of s-cycles, $\langle N_s \rangle / s$: in Table 2, we tabulate the number of s-cycles for the four important scale factors catalogued in Table 1. Note that self-same quasilattices are examples of fixed points in the torus parameterization; in this context, the number of irreducible s-cycles in the golden ratio case (Case 1) was previously computed in [22, 23].

It is interesting to note that the sequences of numbers in some of the columns in Table 2 already appear as entries in the Online Encyclopedia of Integer Sequences (OEIS) for various different reasons. Here we mention those entries for completeness and in the hope that, by tracking down the relationships, some interesting insights might be uncovered. The first column is OEIS sequence A000045 ("Fibonacci numbers"); the second column is A006206 ("Number of aperiodic binary necklaces of length n with no subsequence 00, excluding the necklace "0"); the third column is A000129 ("Pell numbers"); the fourth column is A215335 ("Cyclically smooth Lyndon words with 3 colors"); the fifth column is A001353; the sixth column is A072279 ("Dimension of n-th graded section of a certain Lie algebra"); the seventh column is A001076 ("Denominators of continued fraction convergents to sqrt(5)"); and the eighth column is not yet an OEIS sequence.

s	F_s [2]	$\langle N_s\rangle/s$	F_s	$\langle N_s\rangle/s$	F_s	$\langle N_s\rangle/s$	F_s	$\langle N_s\rangle/s$
1	1	0	1	1	1	2	1	3
2	1	1	2	2	4	5	4	7
3	2	1	5	4	15	16	17	24
4	3	1	12	7	56	45	72	76
5	5	2	29	16	209	144	305	272
6	8	2	70	30	780	440	1292	948
7	13	4	169	68	2911	1440	5473	3496
8	21	5	408	140	10864	4680	23184	12920
9	34	8	985	308	40545	15600	98209	48792
10	55	11	2378	664	151316	52344	416020	185912
11	89	18	5741	1476	564719	177840	1762289	716472
12	144	25	13860	3248	2107560	608160	7465176	2781600

Table 2. Here we list tabulate the first 12 terms in the sequence F_s and the sequence $\langle N_s\rangle/s$, for each of the four important scale factors catalogued in Table 1: $\phi = (1+\sqrt{5})/2$ (columns 1 and 2); $(1+\sqrt{2})$ (columns 3 and 4); $(2+\sqrt{3})$ (columns 5 and 6); and $(2+\sqrt{5})$ (columns 7 and 8).

6 Higher quasilattices

In this paper, we have so far focused on quadratic 1D quasilattices – these form the simplest class of 1D quasilattices, and include the 1D quasilattices needed to build Ammann patterns in two dimensions and higher [12]. Nevertheless, there are also good reasons to think about "higher" 1D quasilattices – *i.e.* 1D quasilattices of degree N (with $N > 2$), and so we briefly consider them in this final section.

We leave a more complete discussion of the degree-N generalization to future work, and here just mention the first few steps. Generalizing Subsection 2.1, we begin by choosing a line $\vec{q}(t)$, an N-dimensional lattice Λ, and an integer basis $\{\vec{m}_1, \ldots, \vec{m}_N\}$ for Λ (with dual basis $\{\widetilde{m}^1, \ldots, \widetilde{m}^N\}$). We take the basis to be "positive" in the sense that it satisfies conditions (2.5a) and (2.5b) for $i = 1, \ldots, N$. Generalizing Subsection 2.2, we see that the intersection of the line $\vec{q}(t)$ with the integer grid of hyperplanes defined by the basis $\{\vec{m}_1, \ldots \vec{m}_N\}$ defines a natural 1D N-grid. In particular, the grid hyperplane whose kth coordinate (in the $\{\vec{m}_1, \ldots, \vec{m}_N\}$ basis) is the integer $n \in \mathbb{Z}$ intersects $\vec{q}(t)$ at $t = t_n^{(k)}$ where

$$t_n^{(k)} = \frac{n - \widetilde{m}^k \vec{q}(t)}{\widetilde{m}^k \hat{e}_\parallel}. \tag{6.1}$$

[Compare with Eqs. (2.6a, 2.6b).] Dualizing this N-grid leads to the quasilattice

$$x = \left\lfloor \widetilde{m}^1 \vec{q}(t) \right\rfloor m_1^\parallel + \ldots + \left\lfloor \widetilde{m}^N \vec{q}(t) \right\rfloor m_N^\parallel + C \tag{6.2}$$

where

$$C = \frac{1}{2}m_1^\parallel + \ldots + \frac{1}{2}m_N^\parallel - q_0^\parallel. \tag{6.3}$$

[Compare with Eqs. (2.7, 2.8).] Generalizing Subsection 2.3, we note that this quasilattice may be reinterpreted as coming from a cut-and-project algorithm, where the integer grid

of hyperplanes defined by the basis $\{\vec{m}_1, \ldots, \vec{m}_N\}$ slices up N-dimensional Euclidean space into N-dimensional parallelopipeds with edges $\{\vec{m}_1, \ldots, \vec{m}_N\}$; and whenever the "cut" line $\vec{q}(t)$ intersects one of these parallelopipeds, we orthogonally project the midpoint of that parallelopiped onto the cut line to obtain the point $\vec{q}(x)$.

It seems particularly interesting to study the subset of these degree-N 1D quasilattices that are self-similar or self-same. Moreover, in our forthcoming paper [12], we will see that a certain subset of these higher 1D quasilattices may be of particular interest as building blocks for novel "higher Ammann patterns" in 2D.

A   Non-negativity of τ

In this Appendix, we prove the assertion from Section 3: that if $\{\vec{m}_1, \vec{m}_2\}$ and $\{\vec{m}_1', \vec{m}_2'\}$ are both *positive* integer bases for Λ and, without loss of generality, we take the $\{\vec{m}_1, \vec{m}_2\}$ parallelogram to be wider than the $\{\vec{m}_1', \vec{m}_2'\}$ parallelogram in the $\hat{e}_\perp$ direction, then the components $\{a, b, c, d\}$ of the 2×2 integer matrix τ are non-negative.

We can prove this as follows. The positivity of the basis $\{\vec{m}_1, \vec{m}_2\}$ implies that $m_1^\parallel$ and $m_2^\parallel$ are both positive, while $m_1^\perp$ and $m_2^\perp$ have opposite signs from one another; and, similarly, the positivity of the basis $\{\vec{m}_1', \vec{m}_2'\}$ implies that $m_1^{\parallel\prime}$ and $m_2^{\parallel\prime}$ are both positive, while $m_1^{\perp\prime}$ and $m_2^{\perp\prime}$ have opposite signs from one another. Furthermore, for the purposes of this proof, we can restrict to the case $m_1^\perp < 0$ and $m_2^\perp > 0$ (since the other possibility corresponds to swapping $1 \leftrightarrow 2$, which just swaps the columns of τ, and does not affect the question of whether its components are all non-negative); and, similarly, we can restrict to the case $m_1^{\perp\prime} < 0$ and $m_2^{\perp\prime} > 0$ (since the other possibility corresponds to swapping $1' \leftrightarrow 2'$, which corresponds to swapping the rows of τ, which again does not affect the question of whether its components are all non-negative). With these restrictions, the requirement $\det(\tau) = \pm 1$ reduces to the condition

$$\det(\tau) = 1, \tag{A.1a}$$

and the requirement that the $\{\vec{m}_1, \vec{m}_2\}$ parallelogram is wider than the $\{\vec{m}_1', \vec{m}_2'\}$ parallelogram in the $\hat{e}_\perp$ direction reduces to the condition

$$m_2^\perp - m_1^\perp > m_2^{\perp\prime} - m_1^{\perp\prime}. \tag{A.1b}$$

Now, using $\vec{m}_1' = a\vec{m}_1 + b\vec{m}_2$, we see that the conditions $m_1^{\parallel\prime} > 0$ and $m_1^{\perp\prime} < 0$ become

$$a > -(m_2^\parallel/m_1^\parallel)b \qquad \text{and} \qquad a > -(m_2^\perp/m_1^\perp)b. \tag{A.2a}$$

In other words, a is greater than both (negative) $\times b$ and (positive) $\times b$, which is only possible if $a > 0$. Similarly, using $\vec{m}_2' = c\vec{m}_1 + d\vec{m}_2$, the conditions $m_2^{\parallel\prime} > 0$ and $m_2^{\perp\prime} > 0$ become

$$d > -(m_1^\parallel/m_2^\parallel)c \qquad \text{and} \qquad d > -(m_1^\perp/m_2^\perp)c, \tag{A.2b}$$

which together imply $d > 0$.

Next, conditions (A.1a) and (A.1b) may be rewritten, respectively, as

$$bc = ad - 1 \tag{A.3a}$$

and
$$bm_2^\perp - cm_1^\perp > (d-1)m_2^\perp - (a-1)m_1^\perp \tag{A.3b}$$

Using the fact that $m_2^\perp$ is positive, $m_1^\perp$ is negative, while a and d are both positive integers, we see that Eqs. (A.3a) and (A.3b) together imply that b and c are both non-negative.

This completes the proof.

B Singular quasilattices

To describe quasilattices and their self-similarity transformations by a formula that continues to be precisely correct even in the singular case (see Sections 2 and 4), we must replace Eqs. (4.5a, 4.5b, 4.5c) by

$$\frac{x_{n,s}}{\lambda_\parallel^2} = \left(\left[\frac{nm_2^\perp - q_{0,s}^\perp}{m_2^\perp - m_1^\perp}\right]_{\sigma_{1,s}} + \frac{\sigma_{1,s}}{2}\right)m_1^\parallel + \left(\left[\frac{nm_1^\perp - q_{0,s}^\perp}{m_1^\perp - m_2^\perp}\right]_{\sigma_{2,s}} + \frac{\sigma_{2,s}}{2}\right)m_2^\parallel - q_{0,s}^\parallel \tag{4.5a$'$}$$

$$= m_1^\parallel(n - \chi_{1,s}^\parallel) + (m_2^\parallel - m_1^\parallel)\left(\left[\kappa_1(n - \chi_{1,s}^\perp)\right]_{\sigma_{2,s}} + \frac{\sigma_{2,s}}{2}\right) \tag{4.5b$'$}$$

$$= m_2^\parallel(n - \chi_{2,s}^\parallel) + (m_1^\parallel - m_2^\parallel)\left(\left[\kappa_2(n - \chi_{2,s}^\perp)\right]_{\sigma_{1,s}} + \frac{\sigma_{1,s}}{2}\right) \tag{4.5c$'$}$$

where
$$\sigma_{1,s} \equiv (\det\tau)^s\sigma_1 \qquad \text{and} \qquad \sigma_{2,s} \equiv (\det\tau)^s\sigma_2. \tag{B.1}$$

Here σ_1 and σ_2 are $\pm$ signs which may be regarded as independent in Eq. (4.5a$'$), but are assumed to obey $\sigma_1 = -\sigma_2$ in passing to Eqs. (4.5b$'$, 4.5b$'$). Also note that we have introduced the notation
$$[x]_\sigma = \begin{cases} \lfloor x \rfloor & (\sigma = +) \\ \lceil x \rceil & (\sigma = -) \end{cases} \tag{B.2}$$

where $\lfloor x \rfloor$ is the "floor" of x (i.e. the greatest integer $\leq x$) and $\lceil x \rceil$ is the "roof" of x (i.e. the least integer $\geq x$).

In particular, note that the "old" self-similarity transformation (4.5b, 4.5c) corresponds to a fixed decoration/gluing rule *except* in the singular case (where the gluing/decoration rule hold *almost* everywhere, but is violated near the singular point in the quasilattice). By contrast, the "new" self-similarity transformation (4.5b$'$, 4.5c$'$) corresponds to a fixed decoration/gluing rule that applies everywhere, even in the singular case.

References

[1] R. Penrose, "The role of aesthetics in pure and applied mathematical research," Bull. Inst. Math. Appl. **10**, 266 (1974).

[2] M. Gardner, "Extraordinary nonperiodic tiling that enriches the theory of tiles," Sci. Amer. **236**, 110 (1977).

[3] R. Penrose, "Pentaplexity," Eureka **39**, 16 (1978).

[4] D. Levine and P.J. Steinhardt, "Quasicrystals: A New Class of Ordered Structures," Phys. Rev. Lett. **53**, 2477 (1984).

[5] B. Grunbaum and G. C. Shephard, *Tilings and Patterns*, W.H.Freeman and Company, New York (1987).

[6] C. Janot, *Quasicrystals*, Oxford University Press, Oxford (1994).

[7] M. Senechal, *Quasicrystals and Geometry*, Cambridge University Press, Cambridge (1995).

[8] M. Baake, "A Guide to Mathematical Quasicrystals," arXiv:math-ph/9901014.

[9] W. Steurer and S. Deloudi, *Crystallography of Quasicrystals: Concepts, Methods and Structures*, Springer-Verlag, Berlin (2009).

[10] M. Baake and U. Grimm, *Aperiodic Order. Volume 1: A Mathematical Invitation*, Cambridge University Press, Cambridge (2013).

[11] M. Senechal, "The Mysterious Mr. Ammann," The Mathematical Intelligencer **26**, 10 (2004).

[12] L. Boyle and P.J. Steinhardt, "Coxeter Pairs, Ammann Patterns and Penrose-like Tilings," arXiv:1608.08215.

[13] N. G. de Bruijn, "Sequences of zeros and ones generated by special production rules," Indagationes Mathematicae (Proceedings), bf 84, 27 (1981).

[14] E. Bombieri and J. E. Taylor, "Which distributions of matter diffract? An initial investigation," J. Phys. Colloques **47**, 19 (1986).

[15] E. Bombieri and J. E. Taylor, "Quasicrystals, Tilings, and Algebraic Number Theory: Some Preliminary Connections," in *The Legacy of Sonya Kovalevskaya*, Cambridge, MA (L. Keen, ed.) Contemp. Math. **64**, 241 (1987), Amer. Math. Soc., Providence, RI.

[16] A. Hof, "On Diffraction by Aperiodic Structures," Commun. Math. Phys. **169**, 25 (1995).

[17] F. J. Dyson, "Random Matrices, Neutron Capture Levels, Quasicrystals and Zeta-function Zeros," Talk given at MSRI Workshop on Random Matrix Theory (2002).

[18] N. P. Fogg, *Substitutions in Dynamics, Arithmetics and Combinatorics*, Springer-Verlag, Berlin (2002).

[19] J.-P. Allouche and J. Shallit, *Automatic Sequences*, Cambridge University Press, Cambridge (2003).

[20] L. Boyle and P.J. Steinhardt, "On Topological Defects in Ammann Patterns and Penrose-like Tilings" (in preparation).

[21] J. E. S. Socolar and P. J. Steinhardt, "Quasicrystals. II. Unit-cell configurations," Phys. Rev. B **34**, 617 (1986).

[22] M. Baake, J. Hermisson and P.A.B. Pleasants, "The torus parameterization of quasiperiodic LI-classes," J. Phys. A **30**, 3029 (1997).

[23] J. Hermisson, C. Richard and M. Baake, "A guide to the symmetry structure of quasiperiodic tiling classes,' J. Phys. I (France) **7**, 1003 (1997).

[24] L. Boyle and P.J. Steinhardt, "Reflection Quasilattices and the Maximal Quasilattice," Phys. Rev. B **94**, 064107 (2016) [arXiv:1604.06426].

[25] J. E. S. Socolar, "Simple octagonal and dodecagonal quasicrstyals," Phys. Rev. B **30**, 10519 (1989).